Performance and stability of semitransparent OPVs for building integration: A benchmarking analysis

D. Chemisana [a *], M. Polo [b], A. Domènech [a], C. Aranda [b], A. Riverola [a], E. Ortega [b], A. Moreno [a], G. Blanco [b], Chr. Lamnatou [a], A. Cot [b]

[a] Applied Physics Section of the Environmental Science Department, University of Lleida, c/Pere Cabrera s/n, 25001 Lleida, Spain

[b] COMSA CORPORACIÓN, Av. Roma, 25-27, 08029 Barcelona, Spain

Abstract: The research presents the experimental performance of three different building-integrated organic semitransparent photovoltaic technologies (A: developed in the present study; B and C: commercial modules). Spectral transmittance and electrical measurements have been conducted in order to determine the characteristics of the modules for building integration and electric generation purposes. Continuous monitoring of the modules working at maximum power point has been performed over sunny days, whereas in other conditions, the modules were kept in open-circuit. Regarding the transmittance, technology A outperforms B and C, but concerning electrical efficiency, C is the one registering the best results in terms of degradation, B is the one achieving the highest efficiencies and A is in the middle (it presents similar efficiency results to C and similar efficiency reduction to B).

1. Introduction

In conventional crystalline photovoltaic installations, the solar cells are responsible for the highest cost, not only from economical point of view but also from environmental perspective. In this regard, organic photovoltaic systems (OPVs) have shown an increasing interest as a cost-effective technology in recent years (Yu et al., 2014). In addition, resources and processes involved in OPV manufacturing and recycling are expected to demand less energy inputs and in this way, OPVs are expected to be more environmentally friendly in comparison to other types of PV systems which include cells with high environmental impact. Moreover, OPVs can be fabricated as thin films, lightweight and flexible modules, widening the possible applications in comparison with conventional silicon PV panels.

Concerning electrical performance, remarkable advances have been reported by utilizing bulk heterojunction organic devices that combine donor and acceptor substances in the blend (Bristow and Kettle, 2015). At present, the efficiency record of 11.7% is held by a team from the Hong Kong University of Science and Technology (Zhao et al., 2016). This impressive value, even to be very high in terms of OPVs, is quite far from the percentages obtained by silicone cells (above 20%). Although the efficiency trend is quite optimistic, stability and large-scale production issues are not as advanced as the efficiencies (Wang et al., 2012). Currently, an important research effort is conducted regarding stability and degradation of organic cells (Ding et al., 2016; Hansson et al., 2016). Degradation mechanisms can be influenced by several factors such as oxidation or hydration/hydrolysis that affect the active layer and the electrodes, diffusion of the electrode materials towards the active layer, etc., and usually is the combination and interrelation between those factors which arise difficulties in

* Corresponding author. E-mail address: daniel.chemisana@macs.udl.cat

understanding the degradation process (Grossiord et al., 2012). Despite the above mentioned drawbacks, a recent study indicates that OPVs with short lifespans of 3 years and efficiencies around 2% are competitive against conventional PV technologies and can produce electricity at around 0.19 €/kWh (Mulligan et al., 2014).

Based on the described characteristics of OPVs regarding the lightweight, flexibility, cost-effectivity, etc., a really feasible application of such technology is for building integration purposes. In this way, an extra value is added since the electrical energy is produced *in situ*. The present study focuses on the benchmarking of three types of OPV modules, two commercially available modules and a module developed in the frame of the SOLPROCEL European project (Solprocel, 2016). All the modules are semitransparent in order to enhance building integration features by allowing daylighting into the interior spaces of a building.

2. Experimental set-up

Spectral and electrical measurements have been carried out to determine the efficiency, transparency and stability of such technologies operating under real conditions, by connecting the modules to a specially designed and manufactured maximum power point tracker (MPPT). A monitoring, from the end of July to the beginning of December (2016,University of Lleida, Lleida, Spain) with at least one month per module, of the MPP electric output has been performed jointly with daily measurements of the intensity-voltage (I-V) curve and spectral transmittance measurements throughout the experimental campaign.

The OPVs assessed were installed facing south in the outdoor testing unit shown in Fig. 1. The OPVs are enclosed in a double glass structure in order to better emulate the real building integration and to keep them flat. As it can be seen in the picture, at the middle of the modules, a pyranometer (Kipp&Zonen CMP6) is placed to register the proper global irradiance received. In addition, every module has attached a T-type thermocouple at its rear part. In the interior space of the testing unit, the MPPTs jointly with the Data Acquisition Systems, DAQs (Campbell Sci.) and the I-V tracer (Keithley 2460) are situated.

Fig. 1. The outdoor testing unit (University of Lleida, Spain).

The MPPT system has been specially designed as this condition is fulfilled in a real installation when the photovoltaic systems are either connected to batteries with a

charge regulator or to the grid with an inverter, but not commercial MPP trackers are available for the ranges of currents and potentials of the assessed modules. Also the built circuit allows acquiring data at any time interval and offers higher flexibility, for example, it automatically switches for measuring the I-V curves.

3. Characterization of the OPV modules

As it was previously indicated, the characterization of the organic modules consists of two types of tests: on one hand, the spectral transmission which determines the lighting abilities of the technologies and, on the other hand, their electrical performance which leads to reliability and suitability features as generation system. As it was mentioned in section 1, the tests were conducted for two OPV semitransparent technologies. The modules developed during the project are named as Technology A (2 modules tested), and the commercial ones as Technology B (2 modules tested) and Technology C (1 module tested).

3.1 Spectral transmission

In order to evaluate the spectral transmission of the OPVs, it is important to introduce the photopic sensitivity curve (Judd, 1951) which ranges from 400 to 700 nm with its peak at 555 nm. This bandwidth comprises the interval wavelength where the transmission of the OPV should be enhanced to allow a proper vision in the interior spaces. In Figure 2, the photopic curve is presented.

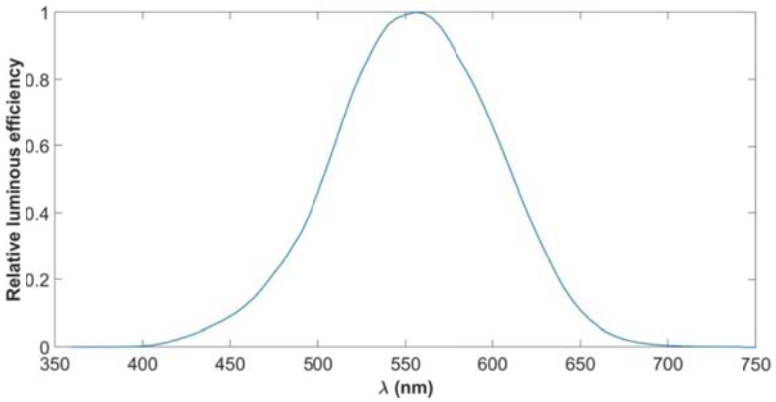

Fig. 2. Photopic sensitivity curve.

For the spectral transmission characterization, an Ocean Optics spectrometer has been used, measuring the spectrum transmitted at 5 different points distributed along the module surface (to determine the homogeneity of the organic blend). As pointed out previously, due to the high flexibility of the photovoltaic elements and in order to better emulate the building-integration conditions, the modules were encapsulated in an extra clear double glass sandwich to keep them flat and also to perform the function of the structural element. To estimate more precisely the transmission of the OPV photovoltaic units, the double glass transmission that supports therein each type of technology is measured. The obtained transmittance values for the photopic range are 86.4%, 85.5% and 84.2% for the technology A, B and C encapsulations respectively.

Fig. 3 plots the 5-sampling points mean spectral transmittance (corrected with the double glass transmittance) for each module technology measured at the end of the characterization. In general, for the measured spectra, small changes are appreciated

regarding the spectral content transmitted. Specifically for the photopic range, the shape of the spectral transmission between the initial measurements and the final measurements is very similar and the variations seem to be negligible. As it can be appreciated in Fig. 3, in the bandwidth 400-700 nm the performance of both technologies is quite stable and lower than that observed from 700 nm on. Conversely, for module C the spectrum presents a quite flat shape for all the range.

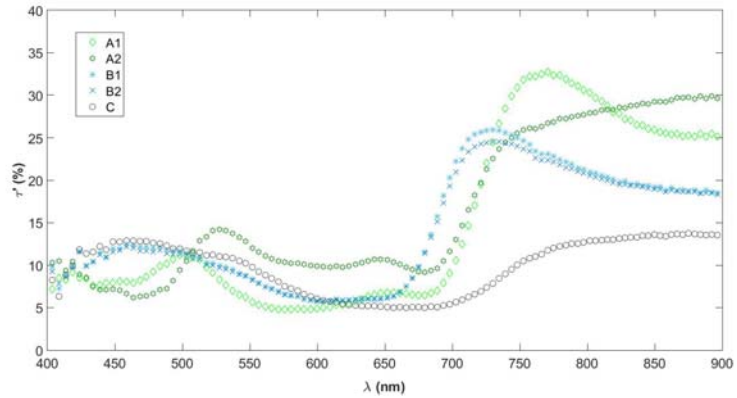

Fig. 3. Mean spectral transmittances of the modules at the end of the monitoring period.

Table 1 includes the mean transmittances of all the modules A, B and C for two different spectral ranges: the first refers to the photopic range (400-700 nm) and the second has been extended till 800 nm considering all the visible bandwidth. Concerning the transmittances, these are reported for two cases: with double glazing ($\bar{\tau}$) and without double glazing ($\bar{\tau}'$). Also the subscripts i and f denote the values measured at the beginning and at the end of the experiments, respectively. From the data it can be pointed out that small variations of the spectral transmittance are registered over the monitoring and that technology A presents higher transmittances (in both ranges considered) than the commercial technologies B and C. Specifically for 400-800 nm bandwidth, technology A results in transmittances ($\bar{\tau}'$) of 12.8% and 12.5% at the beginning and at the end of the time period of the experiments whereas technology B values are 11.5% and 10.5%, analogously. In the case of C, the transmittance decreases in 3.6% points for 400-800 nm interval, but for the range 400-700 nm the values observed are almost equal between the beginning and the end time period (8.2% and 7.8%).

Table 1. Spectral transmission values.

Tech.	$\bar{\tau}_{i\ 400\text{-}700}$ (%)	$\bar{\tau}_{i}'_{400\text{-}700}$ (%)	$\bar{\tau}_{f\ 400\text{-}700}$ (%)	$\bar{\tau}_{f}'_{400\text{-}700}$ (%)	$\bar{\tau}_{i\ 400\text{-}800}$ (%)	$\bar{\tau}_{i}'_{400\text{-}800}$ (%)	$\bar{\tau}_{f\ 400\text{-}800}$ (%)	$\bar{\tau}_{f}'_{400\text{-}800}$ (%)
A1	4.3	4.9	5.4	6.2	9.7	11.2	9.6	10.9
A2	8.1	9.3	6.7	7.8	12.4	14.3	9.4	14.2
B1	6.0	7.0	5.1	5.9	10.5	12.2	9.1	10.6
B2	5.5	6.4	4.7	5.4	9.4	10.9	8.9	10.4
C	6.9	8.2	6.7	7.8	9.5	11.2	6.4	7.6

3.2 Electrical performance

In the present subsection, the J-V characteristic parameters of the modules are analyzed at the beginning of the monitoring period. The modules have been installed on a two-

axis tracker to determine their electrical parameters under stable solar irradiance conditions. In the case of devices developed in project (A), two determinations have been included to discern between (1) behavior after continuous sunlight exposure of ten minutes (in the following notation, it is indicated as +10 min) and (2) measured at the initial time of the exposure (light soaking effects). The measurement conditions, including global irradiance (Glob), direct irradiance (Dir) and the module temperature (T), are included in Table 2 along with a summary of the main electrical parameters determined (J_{sc}: short-circuit current density, V_{oc}: open-circuit potential, FF: fill factor and Ef: efficiency).

Table 2. Summary of the main electrical parameter and the boundary conditions.

Tech.	T (ºC)	Glob (W/m^2)	Dir (W/m^2)	J_{sc} (mA/cm^2)	V_{oc} (V)	FF (%)	Ef (%)
A1	23.22	810	682	0.37	8.75	54.67	2.18
A1(+10min)	24.54	834	705	0.38	8.75	54.82	2.19
A2	21.21	783	672	0.34	8.84	52.92	2.03
A2(+10min)	23.81	802	675	0.35	8.90	52.99	2.06
B1	29.08	1007	875	0.99	8.12	59.19	4.72
B2	29.11	1007	874	1.00	7.59	57.57	4.34
C	30.93	1012	889	0.19	39.28	44.32	3.27

Technology A has been fabricated by utilizing a novel production system based on spraying, which is less expensive and easier than those relying on vacuum processes. On the contrary, as it can be noticed in Table 2, the efficiency values achieved by technology A are half of the values of the commercial technology B. The main factor which leads to this lower efficiency is the fact that the organic tandem photogenerates half of the short circuit current density produced by B modules (it should be considered that the outdoor irradiance is 25% higher for technology B; thus, assuming a direct proportionality between the irradiance and the short circuit current, the values of A modules should be near 0.45 mA/cm^2). Nonetheless, the commercial technology C outperforms technology A due to the high potential achieved since both the short-circuit current density and the fill factor are lower than for the cases of A and B.

3.3 Continuous monitoring

Once the modules were initially characterized, they were installed in the façade-like outdoor experimental testing unit (described in section 2) to start the continuous daily monitoring for sunny days. When the days were cloudy, during the weekends and on holidays (2 weeks in August) the modules were kept in open circuit conditions. Fig. 4 plots the global irradiance evolution throughout the monitoring, where it is possible to notice the increase of irradiance due to the seasonal lower solar altitude effect approaching the winter solstice.

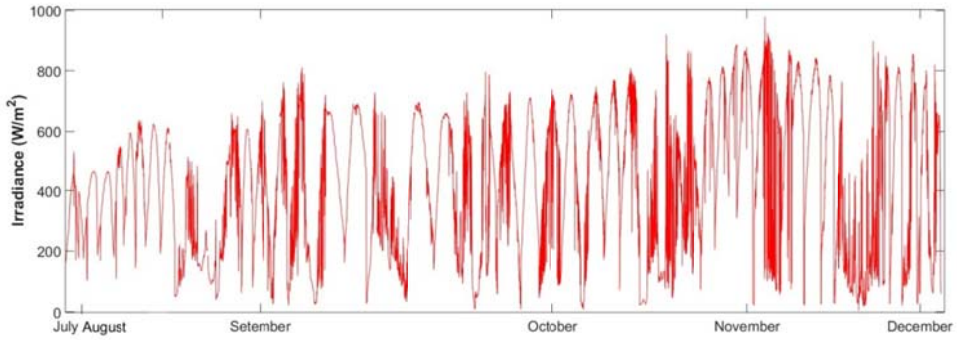

Fig. 4. Global irradiance profile at the plane of the modules.

In the following graphs, some representative results of the modules are included to illustrate how they perform. Firstly, the maximum power output for A modules is included in Fig. 5. It can be seen that both modules present similar tendency, decreasing the power output quite strongly at the first half of the monitoring and stabilizing the reduction at the second half. This appreciation is supported by the efficiency evolution depicted in Fig. 6.

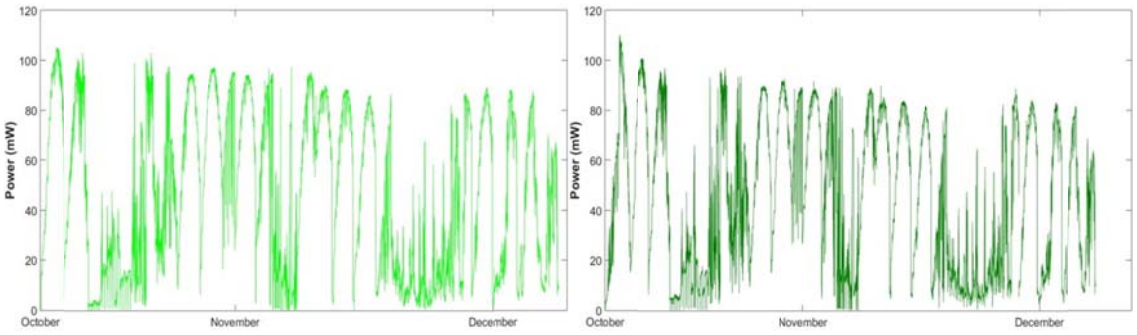

Fig. 5. Maximum power output for module A1 (left) and A2 (right).

Fig. 6a shows the efficiency evolution observed in the case of module A2 (for A1 analogous results were obtained). The efficiency values plotted, measured with the I-V tracer, were previously filtered eliminating all with irradiance values lower than 450 W/m^2 to facilitate comprehension and attending to the fact that those points registered more noise. A quadratic polynomial fitting is applied denoting that, as indicated above, the efficiency reduction decelerates considerably for the second half of the monitoring. This effect was expected by the SOLPROCEL-project partners.

In the case of technology B, the efficiency reduction over the period is more linear than in the case of A modules. The efficiency evolution of module B1 is charted in Fig. 6b. The points included, as in the case of Fig. 6a, were measured with the I-V tracer and a post-processing was applied for selecting values with incident irradiances higher or equal than 450 W/m^2.

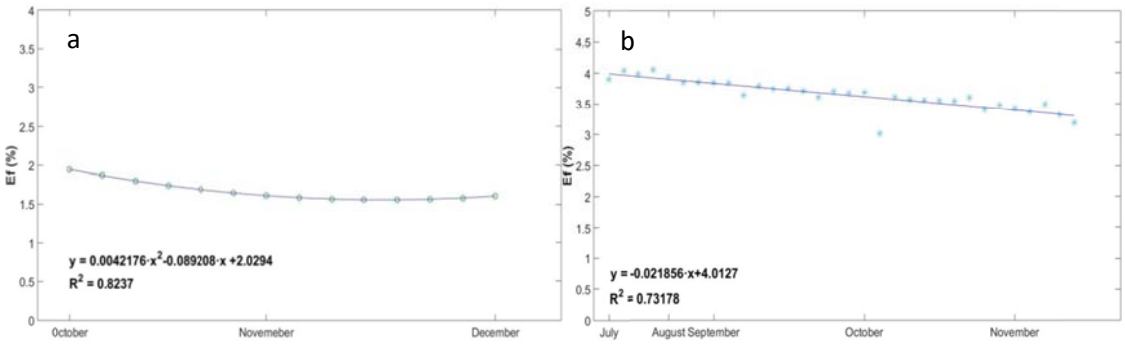

Fig. 6. Efficiency evolution for module A2 (a) and B1 (b).

Finally, Fig. 7 shows the efficiency evolution for module C, but in this case all the measurements conducted with the I-V tracer are included and the fitting is applied only to those obtained with irradiances higher or equal than 450 W/m^2. Technology C is the one achieving the lower efficiency reduction with an almost flat tendency.

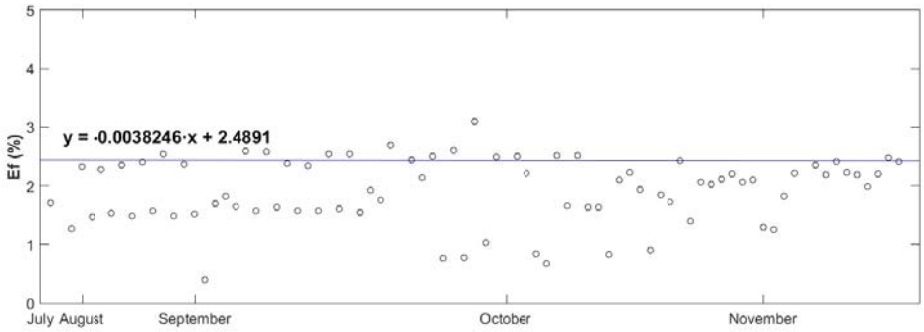

Fig. 7. Efficiency evolution for module C.

In Table 3, the electrical efficiencies at the beginning (i) and at the end (f) of the experimental campaign are summarized. The highest efficiency reduction is suffered by technology A, although this reduction is observed to decrease with much lower rhythm at the second half of the monitoring. Also the calculated differences are not far from those reported for technology B modules. Module C, as it has been noticed in the previous figures, is the one achieving the lowest efficiency reduction.

Table 3. Summary of the electrical efficiencies.

	A1	A2	B1	B2	C
Ef_i (%)	2.083	1.944	3.991	3.722	2.569
Ef_f (%)	1.712	1.607	3.396	3.289	2.477
Relative difference (%)	-17.81	-17.33	-14.90	-11.63	-3.581

6. Conclusions

A benchmarking of three different organic semitransparent technologies, the technology developed in SOLPROCEL project and two commercial ones, has been conducted in order to analyze and compare their efficiency, transparency and stability in a building façade environment.

Regarding transmittance, small variations have been registered over the monitoring and technology A presents higher transmittances in both ranges considered (400-700 nm and

400-800 nm) than the commercial technologies B and C. Specifically for 400-800 nm bandwidth, technology A results in 12.8% and 12.5% at the beginning and at the end of the time period of the experiments whereas technology B values are 11.5% and 10.5%, analogously. In the case of C, the transmittance decreases in 3.6% points for 400-800 nm interval, but for the range 400-700 nm the values observed are almost equal between the beginning and the end time period (8.2% and 7.8%).

The electrical efficiency values achieved by technology A are half of the values of the commercial technology B. The main factor which leads to this lower efficiency is the fact that the organic tandem photogenerates half of the short-circuit current density of B modules. Nonetheless, the commercial technology C outperforms technology A due to the high potential achieved as both the short-circuit current density and the fill factor are lower than for A and B. The highest efficiency reduction is suffered by technology A whereas this reduction is observed to decrease with much lower rhythm at the second half of the monitoring. Also the calculated differences are not far from those reported for technology B modules. Module C is the one achieving the lowest efficiency reduction (3.6%).

Acknowledgments: The authors would like to acknowledge financial support from European Commission 7th Framework Programme (FP7-NMP-2013-SMALL-7).

7. References

Bristow N.,Kettle J., Outdoor performance of organic photovoltaics: Diurnal analysis, dependence on temperature, irradiance, and degradation. Journal of Renewable and Sustainable Energy, 2015;7(1).

Ding Z., Kettle J., Horie M., Chang S.W., Smith G.C., Shames A.I., et al., . Efficient solar cells are more stable: The impact of polymer molecular weight on performance of organic photovoltaics. Journal of Materials Chemistry A, 2016;4:7274-7280.

Grossiord N., Kroon J.M., Andriessen R., Blom P.W.M., Degradation mechanisms in organic photovoltaic devices. Organic Electronics, 2012;13(3):432-456.

Hansson R., Lindqvist C., Ericsson L.K.E., Opitz A., Wang E., Moons E., Photo-degradation in air of the active layer components in a thiophene-quinoxaline copolymer: fullerene solar cell. Physical Chemistry Chemical Physics, 2016;18:11132-11138.

Judd D. B. (1951), Report of U.S. secretariat committee on colorimetry and artificial daylight, proceedings of the twelfth session of the CIE, Stockholm (pp. 11) Paris: Bureau Central de la CIE.

Mulligan C.J., Wilson M., Bryant G.,Vaughan B., Zhou X., Belcher W.J., Dastoor P.C., A projection of commercial-scale organic photovoltaic module costs. Solar Energy Materials and Solar Cells, 2014;120(Part A):9-17.

Solprocel (2016),www.solprocel.eu

Wang Y., Wei W., Liu X., Gu, Y. Research progress on polymer heterojunction solar cells. Solar Energy Materials and Solar Cells, 2012;98:129-145.

Yu J., Zheng Y., Huang J., Towards high performance organic photovoltaic cells: A review of recent development in organic photovoltaics. Polymers, 2014;6: 2473–2509.

Zhao J., Li Y., Yang G., Jiang K., Lin H., Ade H., et al., Efficient organic solar cells processed from hydrocarbon solvents. Nature Energy 1, Article number: 15027 (2016).